Characterisation Techniques for the Study of Nanoscale Polymeric Systems in Two- and Three-Dimensions

D.J. Stokes, S. Reyntjens, C. Jiao, M.F. Hayles and D.H.W. Hubert

FEI Company, Building AAE, PO Box 80066, 5600 Eindhoven, The Netherlands
Debbie.Stokes@fei.com, Steve.Reyntjens@fei.com, Chengge.Jiao@fei.com, Mike.Hayles@fei.com, Dominique.Hubert@fei.com,

ABSTRACT

The development of polymer-based materials, composites and devices is more intense than ever, and so techniques and methods for their characterisation have become more powerful, giving new insights into the spatial relationships between heterogeneous nanostructures. A case in point is the application of state-of-the-art focused ion beam technology (FIB), in combination with high-performance scanning electron microscopy (SEM), allowing us to generate cross-sections into bulk material and create a series of sequential images. For polymeric systems, this may require the simultaneous use of cryogenic temperatures in order to minimise any structural distortions, and strategies are also required to overcome problems associated with charge build-up when dealing with such electrically insulating specimens. With appropriate software, two-dimensional images can be correlated and volume-rendered into a three-dimensional representation. In addition, site-specific lamellar specimens can be made, for observation in the (scanning) transmission electron microscope (S/TEM), with the advantage that FIB cutting through hard-soft interfaces poses fewer difficulties compared to traditional ultra-microtomy.

Keywords: polymers, FIB SEM, S/TEM, hard-soft, 3D

1 2D STUDIES OF POLYMERIC MATERIALS

This section outlines a number of approaches to imaging polymeric materials utilizing signals generated and collected by a variety of means.

In systems consisting of both FIB and SEM capabilities, there is the option to generate backscattered electron signals (BSE), secondary electron signals (SE) and secondary ion signals (SI). SE signal generation is common to both electron and ion primary beams. BSE are associated only with the electron beam and, likewise, SI to the ion beam.

For electron beam imaging of electrically insulating materials, it is advantageous to operate in a partial pressure of a suitable gas and use electron-gas interactions to compensate for negative charge build up (see section 1.2). To compensate for positive charging during ion beam irradiation, there are methods for applying sources of negative charge [1, 2].

1.1 SEM imaging – high vacuum, low voltage

It is well known that electrically insulating materials are prone to charging in high vacuum conditions and that, for imaging these materials uncoated, low accelerating voltages can be used. In the past, this would have meant compromising on resolution, as low voltage beams are more sensitive to lens aberrations and quality of vacuum for example. Recent technological developments, such as improved lens and detector designs, bring a vast improvement in low kV resolution. For example, an in-lens type of detector allows high resolution backscattered electron (BSE) and secondary electron (SE) imaging, even at low accelerating voltages.

1.2 Low vacuum SEM

Alternatively, imaging in a gaseous environment is well suited to work involving uncoated electrically insulating materials. Ionising collisions of emitted electrons with gas molecules give rise to positive ions that help to mitigate negative charge deposited by the electron beam. Gases that have been used include water vapor, nitrogen, nitrous oxide, carbon dioxide, argon, helium and air (see, for example, [3, 4]).

An additional advantage of this approach is that it allows the use of a greater range of accelerating voltages. This is important when locating and imaging specific features of interest. For example, Figures 2a and 2b show the same field-of-view for a thin polymer film on a copper grid. At high voltages, the electron beam penetrates right through the film, making it seem invisible.

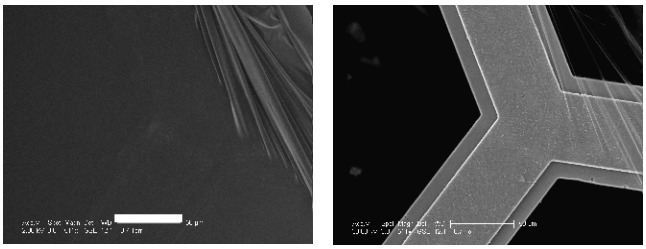

Figure 1 : Same field-of-view of a thin polymer film (~160 nm thickness), spin-cast onto a copper grid. The low voltage (2 kV) image (a) demonstrates that the electron beam is localized at the film surface. At higher voltage (30 kV) beam penetration dominates. Scale bar =50 μm

Conversely, Figure 2 shows other circumstances for which working at higher voltages helps, when imaging at greater depths is needed. Hence, low vacuum mode gives greater flexibility to choose an accelerating voltage appropriate to the information required.

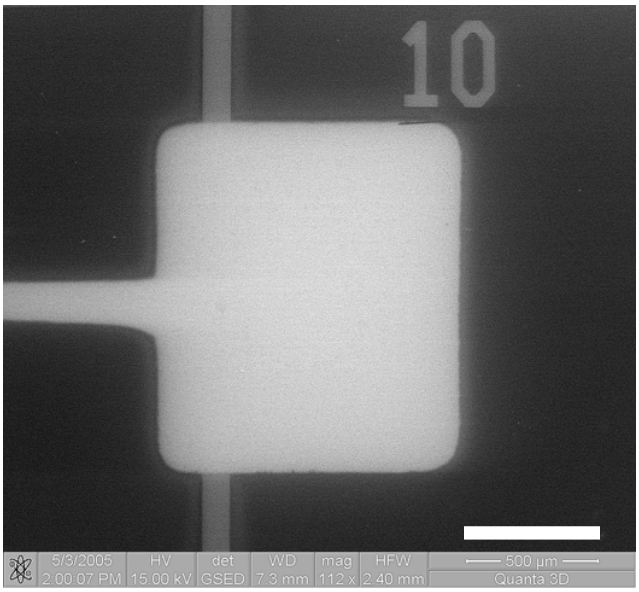

Figure 2a : Low vacuum SE image of part of a semi-conducting polymer transistor (15 kV accelerating voltage). Visible are a gate electrode (upper surface) and some features underlying several thin layers of polymer. Scale bar = 500 µm

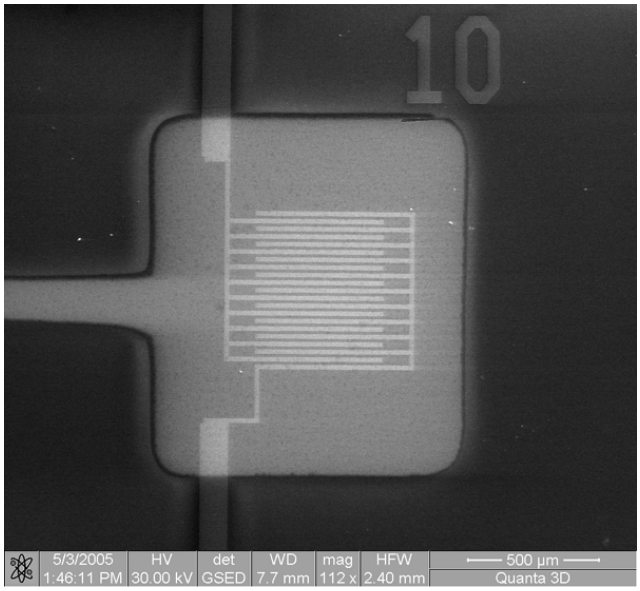

Figure 2b : As for 2a, but imaged at higher accelerating voltage (30 kV). Beneath the upper gate electrode and several polymer layers lies the inter-digitated source-drain region

1.3 STEM-in-SEM

A further imaging mode is that of scanning transmission electron microscopy (STEM), whereby a multi-segment solid-state detector is placed beneath a thin specimen and the transmitted electrons collected to give bright- and dark-field images. The relatively low accelerating voltages used in the SEM mean that high-contrast images are obtained. Figure 3 shows an example of imaging in this mode, in a low vacuum environment.

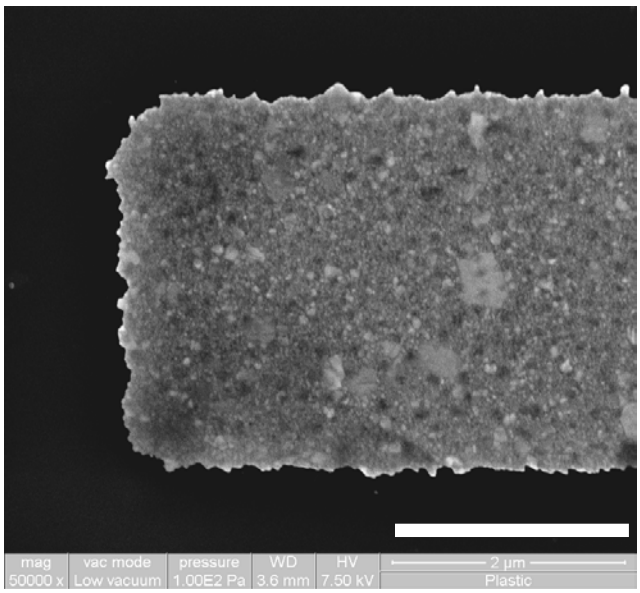

Figure 3 : STEM-in-SEM image of part of a semi-conducting polymer structure, imaged in water vapor at a partial pressure of 100 Pa (~0.75 torr). Scale bar = 2 µm

In addition, x-ray microanalysis can be carried out and, since the interaction volume is very small in thin materials, high resolution results are obtained.

1.4 Focused ion beam-induced imaging

The large size of the ions means that the penetration depth and, hence, interaction volume of the primary ion beam is very much smaller than that for primary electrons. As a result, effects such as channelling contrast in crystalline materials become much more pronounced in ion beam-generated images. This is demonstrated in Figure 4. When the ion beam is incident nearly parallel to a low index crystallographic direction, ions that pass father away from the rows suffer only small angular deflection at each collision. These ions can travel a considerable distance through the crystal before stopping. Channelling reduces the electron yield: electron emission depends on the inelastic energy loss and the channelled ion transfers relatively little energy in each collision along its path.

NSTI-Nanotech 2007, www.nsti.org, ISBN 1420061836 Vol. 2, 2007

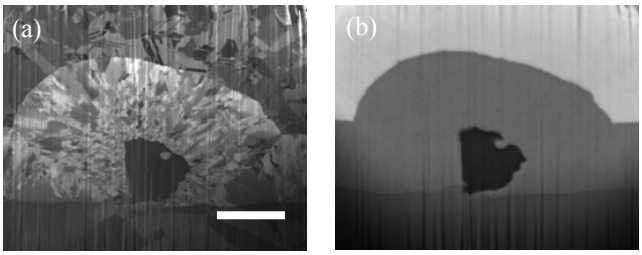

Figure 4 : (a) Ion-induced channeling contrast (secondary ion signal in this case) and (b) backscattered electron image of the same field of view. Scale bar ~ 5 μm

This type of contrast can also be used to distinguish different layers in heterogeneous specimens, such as the packaging material shown in Figure 5. A polycrystalline clay layer is clearly visible within and beneath the polymeric layers.

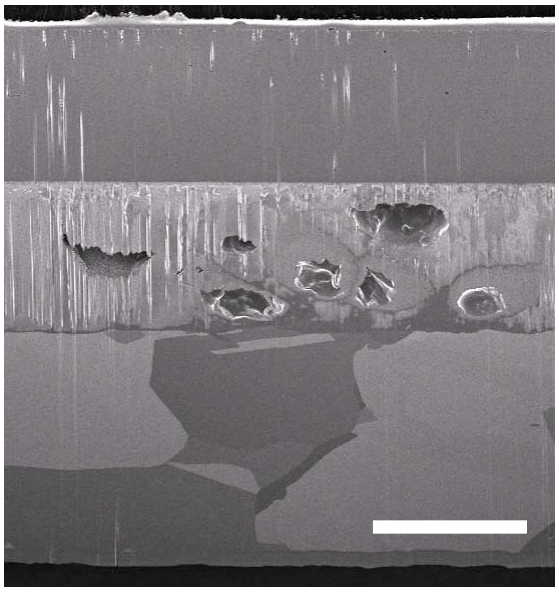

Figure 5 : Ion beam-induced secondary electron image of polymer packaging material with clay barrier layer. Scale bar ~ 10 μm

In this case, a thin lamellar specimen was prepared *in situ* using FIB milling, as described below.

1.5 Focused ion beam-prepared specimens for high-resolution S/TEM

In addition to using the electron and ion beams separately, for imaging, the FIB is primarily used to remove material by sputtering. With the specimen tilted normal to the ion beam, a cross-section can be milled into the bulk material, and an electron image can be obtained without having to move the specimen. Indeed, milling and imaging can take place simultaneously, to monitor progress. The geometry of a typical combined FIB SEM system is illustrated in Figure 6.

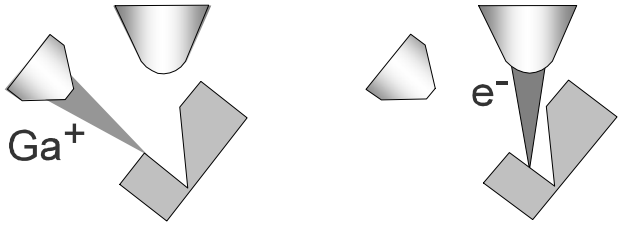

Figure 6 : Schematic diagram showing the relationship between ion and electron columns, and the tilted specimen in a FIB SEM system

This arrangement can be used to make thin lamellar specimens, by milling on either side. Lamellae can be transferred, by various means, onto a grid for S/TEM imaging. Figure 7 shows such a lamella that has been 'lifted out' and placed on a TEM grid (using *in situ* chemical vapor deposition).

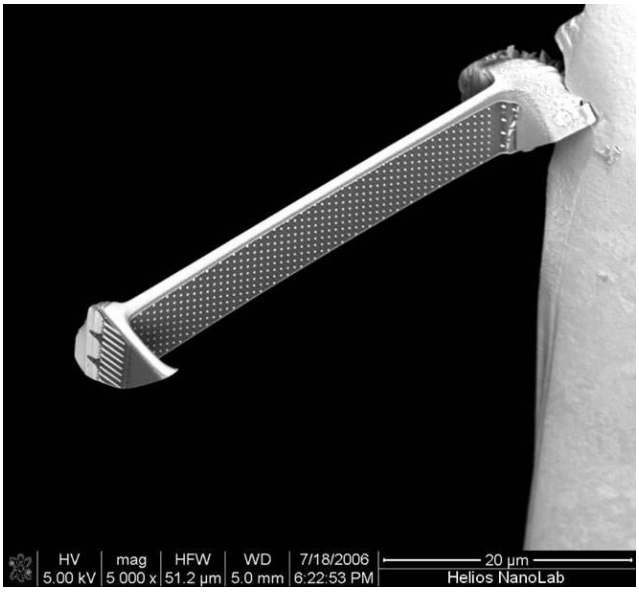

Figure 7 : Example of a FIB-milled lamellar specimen, prepared for subsequent imaging in HR-S/TEM

Loos *et al* [3] successfully used this method to prepare a polymeric solar cell construction, similar to that shown in Figure 8, for observation in high-resolution TEM.

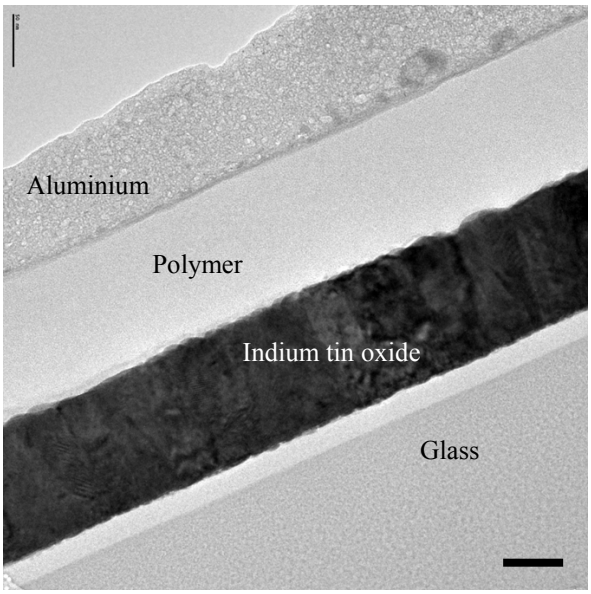

Figure 8 : High-resolution TEM image of FIB-prepared multi-layer lamellar specimen. For details, see ref [1]. Scale bar = 50 nm

2 3D STUDIES OF POLYMERIC SYSTEMS: FIB SEM TOMOGRAPHY

Figure 9 shows a FIB-prepared cross-section through a laminated polymer containing ceramic nanoparticles. In this case, the specimen was frozen using a cryo-transfer system and cryoSEM stage (Quorum PP2000T) to confer rigidity to the delicate structure prior to FIB milling.

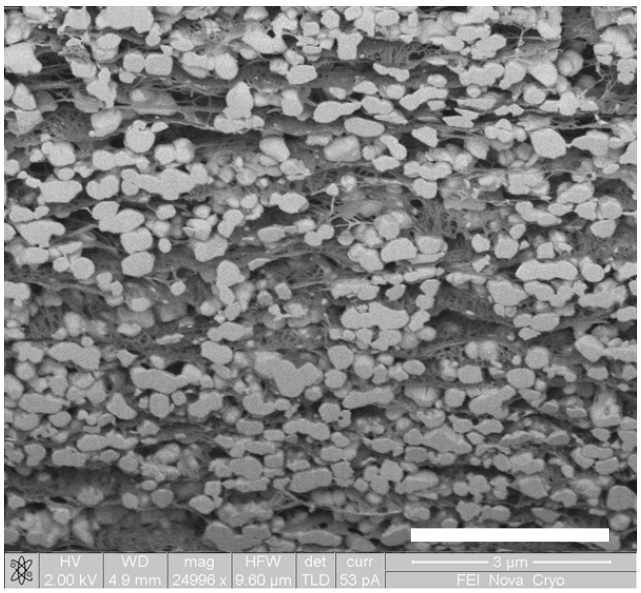

Figure 9 : Ceramic nanoparticles in a laminated polymer matrix, prepared by cryoFIB. Scale bar = 3 µm

With the ability to perform cross-sectioning with the FIB, and then image with the electron beam, it becomes possible to carry out serial sectioning of materials. If the ion beam is moved by regular intervals, a sequence of 2D images (see Figure 10) can be used as the basis for 3D tomographic reconstruction.

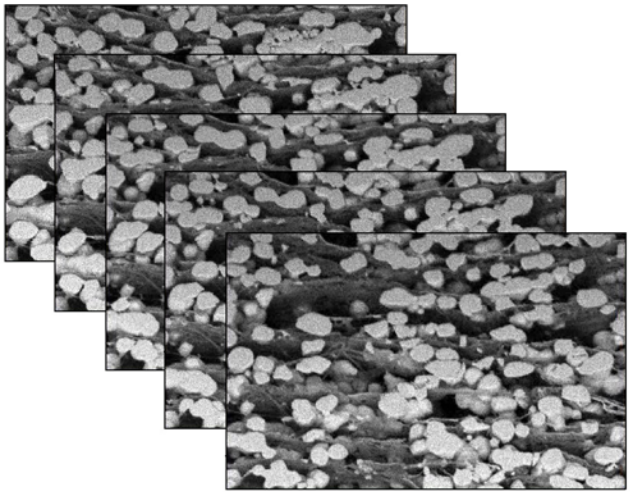

Figure 10: A set of 2D slices, taken at regular intervals, ready for 3D reconstruction. Same specimen as shown in Figure 9 (horizontal field width ~ 2.5 um)

3 CONCLUSIONS

Improvements in detector design and developments in instrumentation, together with versatile specimen preparation methods and data handling techniques, offer a renewed scope for the characterization of soft matter in general, and polymers in particular. These advances are of crucial importance as the technological significance of polymeric materials, systems and devices grows, and their dimensions shrink.

REFERENCES

[1] J. Cazaux. *Journal of Electron Spectroscopy and Related Phenomena* **113**(1) (2000) p. 15-33.
[2] D.J. Stokes, T Vystavel, F. Morrissey. *J. Phys. D: Appl. Phys.* **40** (2007) p. 874-877.
[3] A.L. Fletcher, B.L. Thiel, A.M. Donald. J. Phys. D: Appl. Phys. **30** (1997) p. 2249-2257
[4] Thiel, B.L., et al., *An Improved Model for Gaseous Amplification in the Environmental SEM.* J. Microscopy., 1997. **187**(Pt. 3): p. 143-157.
[5] J. Loos, J.K.J. van Duren, F. Morrissey, R.A.J. Janssen. *Polymer* **43** (2002) p. 7493-7496.